

ImmunoPET and immunoSPECT of rheumatoid arthritis with radiolabeled anti-fibroblast activation protein (FAP) antibody correlates with severity of arthritis

Peter Laverman¹, Tessa van der Geest¹, Samantha Y.A. Terry^{1,2}, Danny Gerrits¹, Birgitte Walgreen³, Monique M. Helsen³, Tapan K. Nayak⁴, Anne Freimoser-Grundschober⁵, Inja Waldhauer⁵, Ralf J. Hosse⁵, Ekkehard Moessner⁵, Pablo Umana⁵, Christian Klein⁵, Wim J.G. Oyen¹, Marije I. Koenders³, Otto C. Boerman¹

¹Department of Radiology and Nuclear Medicine, Radboud University Medical Center, Nijmegen, The Netherlands;

²Department of Imaging Sciences, King's College London, London, United Kingdom;

³Department of Experimental Rheumatology, Radboud University Medical Center, Nijmegen, The Netherlands;

⁴Roche Pharmaceutical Research and Early development, Innovation Center Basel, Basel, Switzerland;

⁵Roche Pharmaceutical Research and Early development, Innovation Center Zurich, Schlieren, Switzerland.

Corresponding author: Peter Laverman, PhD

Radboud University Medical Center, Department of Radiology and Nuclear Medicine

PO Box 9101, 6500 HB Nijmegen, The Netherlands

Phone: +31-24-3615054, E-mail: peter.laverman@radboudumc.nl

Word count: 5014

Disclaimer: Samantha Y.A. Terry was funded by the Roche Postdoc Fellowship (RPF) Program.

Running title: FAP imaging in rheumatoid arthritis

ABSTRACT

One of the most prominent cell populations playing a role in rheumatoid arthritis (RA) is activated fibroblast-like synoviocytes (FLSs). Among many other proteins, FLSs dominantly express fibroblast activation protein (FAP). Due to high expression of FAP in arthritic joints, radioimmunoimaging of activated fibroblasts with anti-FAP antibodies might be an attractive non-invasive imaging tool in RA.

Methods. Single photon emission computed tomography (SPECT) and positron emission tomography (PET) with ^{111}In - and ^{89}Zr -labeled anti-FAP antibody 28H1 was performed in mice with collagen-induced arthritis. Radioactivity uptake in joints was quantified and correlated with arthritis score.

Results. Both ^{111}In -28H1 and ^{89}Zr -28H1 showed high uptake in inflamed joints, being 3-fold higher than that of the irrelevant isotype-matched control antibody DP47GS, clearly indicating specific accumulation of 28H1. Uptake of ^{111}In -28H1 ranged from 2.2 %ID/g in non-inflamed joints to 32.1 %ID/g in severely inflamed joints. DP47GS accumulation ranged from 1.6 %ID/g in non-inflamed tissue to 12.0 %ID/g in severely inflamed joints. Uptake of 28H1 in inflamed joints correlated with arthritis score (Spearman's p 0.69, $p<0.0001$) and increased with severity of arthritis.

Conclusions. SPECT/CT imaging with the anti-FAP antibody ^{111}In -28H1 specifically visualized arthritic joints with high resolution, and tracer accumulation correlated with the severity of the inflammation in murine experimental arthritis. Background uptake of the radiolabeled antibody was low, resulting in excellent image quality. ^{89}Zr -28H1 was less favorable for RA imaging due to an elevated bone uptake of ^{89}Zr . Future studies will focus on the potential role of 28H1 as a tool to monitor therapy response early-on.

Keywords

Fibroblast activation protein (FAP), SPECT imaging, PET imaging, collagen-induced arthritis, monoclonal antibody

INTRODUCTION

Rheumatoid arthritis (RA) is an autoimmune disease that results in chronic and systemic inflammation in synovial joints. RA is characterized by hyperplasia and chronic inflammation of synovial membranes that invade into articular cartilage and bone. Many cell types that play a role in joint destruction are present in the synovial lining layer. One of the most prominent cell populations is activated fibroblast-like synoviocytes (FLSs) which is involved in pannus formation (1). Among many other proteins, FLSs dominantly express fibroblast activation protein (FAP) (2). It has previously been shown that the area where these FAP-expressing FLSs are present corresponds with the center of high inflammatory activity (2).

FAP is a cell surface-bound, type II transmembrane glycoprotein, belonging to the family of serine prolyl oligopeptidases, has a molecular weight of 95 kDa and is abundantly expressed in granulation tissue of healing wounds (3, 4). It has been shown that FAP is closely related to dipeptidylpeptidase IV (DPP IV), also known as CD26 (5). Besides peptidase activity, it was demonstrated that FAP has collagenase activity *in vitro* (6). FAP is also found in more than 90% of human epithelial carcinomas (3, 7), where its expression is limited to fibroblasts in the tumor stroma (8). We hypothesized that, due to high expression of FAP in arthritic joints, radioimmunoimaging of activated fibroblasts with anti-FAP antibodies might be an attractive non-invasive imaging tool in RA.

Since FAP is expressed in tumor stroma, various anti-FAP antibodies have been studied for radioimmunotargeting of malignancies. Amongst these are ¹³¹I-labeled murine F19 (9) and ¹³¹I-labeled sibrotuzumab, a humanized version of the F19 antibody (10). More recently, two new anti-FAP

antibodies, ESC11 and ESC14, were labeled with ^{177}Lu , which showed excellent targeting in melanoma xenografts (11).

In the present study, we investigated the potential of a radiolabeled anti-FAP antibody for specific positron emission tomography (PET) and single photon emission computed tomography (SPECT) of activated fibroblasts in an experimental model of RA. While PET is generally better for quantification purposes, preclinical SPECT imaging has a higher resolution.

Fischer et al. grafted the human anti-FAP Fab fragments into the human IgG1 framework, resulting in fully human anti-FAP IgG1 antibodies (11). Here we used the 28H1 antibody, which is an non-internalizing anti-FAP antibody with high pM affinity for both murine and human FAP and bearing mutations in the Fc part, preventing binding to the Fcy receptors. In brief, the antibody was conjugated with desferal for ^{89}Zr labeling and with diethylene triamine pentaacetic acid (DTPA) to allow ^{111}In labeling. PET/CT and SPECT/CT imaging studies as well as biodistribution studies were performed in mice with collagen-II-induced arthritis (CIA) to correlate the radioactivity concentration in the joints with the severity of arthritis.

MATERIALS AND METHODS

Animals

Male DBA/1J mice were obtained from Janvier-Elevage (Le Genest Saint Isle, France). All mice were housed in filter-top cages under specific pathogen-free conditions and a standard diet and water were provided ad libitum. The mice were used between 10 and 12 weeks of age. All animal procedures were approved by the institutional animal welfare committee and carried out according to their guidelines.

Antibody conjugation and radiolabeling

The monoclonal anti-FAP antibody 28H1 has high avidity for murine (< 1 pM) and human FAP (268 pM) and has the P329G LALA mutations in the Fc part to make it Fc effector silent. The monoclonal antibody DP47GS with the P329G LALA mutations served as an isotype-matched control antibody with no known binding specificity and no affinity for murine nor human FAP. The 28H1 anti-FAP antibody is a fully human FAP antibody that was generated by phage display using recombinant FAP (manuscript in preparation, patent application WO/2012/020006). In order to abolish Fc γ R and C1q binding a P329G LALA mutation was introduced that completely abolishes Fc γ R and C1q binding, but does not affect FcRn binding and pharmacokinetics (manuscript in preparation, patent application: WO/2012/130831).

Both 28H1 and DP47GS were conjugated with isothiocyanatobenzyl-diethylenetriaminepentaacetic acid (p-SCN-Bz-DTPA) (Macrocyclics, Inc., Dallas, TX) according to standard procedures. Labeling with $^{111}\text{InCl}_3$ (Mallinckrodt BV, Petten, The Netherlands) was performed as described previously (12). Labeling efficiencies were >99% and 89% for ^{111}In -DTPA-28H1 and ^{111}In -DTPA-DP47GS, respectively. ^{111}In -DTPA-DP47GS was purified on a PD-10 column (GE Healthcare Biosciences, Uppsala, Sweden), and

eluted with phosphate-buffered saline (PBS), containing 0.5% bovine serum albumin (BSA), to provide two preparations with a radiochemical purity of ≥ 99%.

In addition, the 28H1 antibody was modified with succinyl-desferal-iron-tetrafluorophenol ester (VU University Medical Center, Amsterdam) as described previously (13). The 28H1-desferal conjugate (1 mg) was radiolabeled with 110 MBq of ⁸⁹Zr (PerkinElmer, Boston, MA) in 0.5 M HEPES, pH 7.2, for 60 min at 37°C. Labeling efficiency was 97% as determined by ITLC. The reaction mixture was purified on a PD-10 column eluted with gentisic acid (5 mg/ml). The radiochemical purity of ⁸⁹Zr-N-succinyl-desferal-28H1 (⁸⁹Zr-28H1) was >99%.

[¹⁸F]FDG was purchased as ready-to-use product (GE Healthcare, Eindhoven, the Netherlands).

Binding assay of 28H1

Human fibroblast cell line GM05389 and murine 3T3 fibroblasts stably transfected with murine FAP were detached with Cell Dissociation Buffer and resuspended in FACS buffer. Cells (200,000) were seeded into a 96-well round bottom plate. The plate was centrifuged at 400xg for 3 min to pellet the cells. The supernatant was removed and cells were resuspended in 40 µl of Alexa647-labeled anti-FAP 28H1 or DP47GS at 10 µg/ml. The plate was incubated for 30 min at 4°C to allow binding of the antibodies. To remove unbound antibodies the cells were centrifuged again and washed twice with FACS buffer, resuspended in 200 µl FACS buffer and the fluorescence was measured by flow cytometry.

Animal experiments

For the induction of collagen-induced arthritis, Freund's complete adjuvant (FCA) and Mycobacterium tuberculosis (strain H37Ra) were obtained from Difco, Detroit, MI. Bovine collagen type II (CII) was

prepared as described previously (14). DBA/1J mice were immunized intradermally at the base of the tail with 100 µg of CII. Three weeks later, mice received an intraperitoneal booster injection of 100 µg CII dissolved in PBS. The onset of arthritis occurred a few days after the booster injection. Clinical onset and progression was monitored by macroscopic scoring of the paws, on a scale of 0 to 2 for each paw, in a blinded fashion by two independent observers. Cumulative scoring based on redness, swelling, and, in later stages ankylosis was as follows: 0=no changes; 0.25=1-2 toes red or swollen; 0.5=3-5 toes red or swollen; 1=swollen ankle; 1.5=swollen footpad; 2=severe swelling and ankylosis. Naïve mice, i.e. not immunized, were used as control. Mice were injected with the radiolabeled antibodies at day 24-26 after start of the immunization. SPECT/CT imaging with ¹¹¹In-28H1 and ¹¹¹In-DP47GS was performed as follows. Mice (n=3/group) received an intravenous (i.v.) injection of 15-18 MBq of ¹¹¹In-28H1 or ¹¹¹In-DP47GS (injected dose 50 µg). At 1 and 3 days post injection (p.i.), images were acquired with the U-SPECT-II/CT (MILabs) (15). Mice were scanned under general anesthesia (isoflurane and air) for 60 min (4x 15 min frames) using a 1.0-mm-diameter pinhole Ultra High Sensitivity mouse collimator (UHS-M). One mouse was scanned using a 0.35-mm-diameter pinhole Ultra High Resolution mouse collimator (UHR-M). SPECT scans were followed by CT scans (65 kV, 615 µA). SPECT scans were reconstructed with software from MILabs, which uses an ordered-subset expectation maximization algorithm, with a voxel size of 0.375 mm. Using Inveon Research Workplace software (IAW 4.0, Siemens Preclinical Solutions, Knoxville, TN) a 3D volume of interest was drawn around the arthritic joints, and the uptake was quantified as percentage of the injected dose (%ID). For PET/CT imaging with ⁸⁹Zr-28H1 and [¹⁸F]FDG, mice (n=3/group) received an i.v. injection of 5-7 MBq of ⁸⁹Zr-28H1 (injected dose 50 µg) or 5 MBq [¹⁸F]FDG. For ⁸⁹Zr-28H1, PET/CT images were acquired with the Inveon animal PET scanner (16) (Siemens Preclinical Solutions, Knoxville, TN) under general anesthesia (isoflurane and air) for 20 min at 1 and 3 d p.i.. FDG-PET scans (20 min) were acquired 45 min p.i., while mice remained under general

anesthesia during time between injection and imaging. PET scans were followed by CT scans (80 kV, 500 µA). PET scans were reconstructed using Inveon Acquisition Workplace software (v 1.5, Siemens) using an ordered-set expectation maximization 3-dimensional maximum a posteriori (OSEM-3D MAP) algorithm with the following parameters: matrix, 256 × 256 × 159; pixel size, 0.43 × 0.43 × 0.8 mm; and a uniform-variance maximum a posteriori prior, 0.5 mm. For the biodistribution studies after dissection, mice (n=5/group) with various macroscopic scores of arthritis received an i.v. injection of 370 kBq ⁸⁹Zr-28H1, ¹¹¹In-28H1 or ¹¹¹In-DP47GS (injected dose 50 µg) or 10 MBq [¹⁸F]FDG. At 72 h p.i (⁸⁹Zr-28H1, ¹¹¹In-28H1 or ¹¹¹In-DP47GS) or 1 h p.i. ([¹⁸F]FDG), mice were euthanized by CO₂/O₂ asphyxiation, a blood sample was drawn and tissues of interest were dissected, weighed and counted in a gamma counter. The percentage of the injected dose per gram tissue (%ID/g) was calculated for each tissue. Joints were dissected with minimal residual bone/muscle. Uptake in the joints was correlated with the individual arthritis scores of the joints prior to dissection.

Immunohistochemistry

To demonstrate FAP expression in arthritic murine joints, frozen sections of ankle joints from mice with CIA were stained with monoclonal anti-FAP antibody 28H1 and isotype-matched control DP47GS. Frozen sections of 5 µm were dried overnight at RT and then fixed with ice-cold acetone for 10 min. After drying for at least 1 h at RT the primary antibody 28H1 or DP47GS was applied and incubated for 1 h at RT. After three washing steps with 50 mM PBS, pH 7.4, the secondary antibody goat-anti-human IgG-peroxidase was applied. After 30 min at RT, slides were washed three times with PBS. Finally, the sections were stained for 10 min with diaminobenzidine (DAB) and subsequently for 5 seconds with hematoxilin.

Statistical analysis

All mean values are given \pm standard deviation (S.D.). Unless state otherwise, statistical analysis was performed using a Welch's corrected unpaired Student's t-test or one-way analysis of variance using GraphPad Prism software (version 5.03 GraphPad Software). The level of significance was set at P<0.05.

RESULTS

Immunohistochemistry with 28H1 demonstrated abundant expression of FAP in an inflamed knee joint from a CIA mouse (supplemental figure 1A). Staining with DP47GS was negative (supplemental figure 1B). Staining with 28H1 on knee tissue from a healthy mouse was also negative (supplemental figure 1C). An in vitro binding assay on both human and murine fibroblasts demonstrated high and specific binding to FAP (supplemental data, figure 2).

SPECT/CT imaging

To investigate the feasibility of imaging with anti-FAP antibodies in arthritis, collagen-induced arthritis was induced in DBA/1J mice, and SPECT/CT and PET/CT imaging with anti-FAP antibody 28H1 were performed after clinical onset of arthritis. ^{111}In -28H1 SPECT/CT scans of mice with arthritic joints clearly demonstrated strong accumulation of the anti-FAP antibody in the inflamed joints, with little background activity in other tissues. SPECT with ^{111}In -28H1 delineated all inflamed joints, even joints with minimal arthritic scores (0.25 on a scale of 0-2) as well as small, inflamed joints, such as those in the feet and toes. Lungs were also visible on the SPECT scans at 24 h p.i. (figure 1A), however, this accumulation had disappeared at 72 h p.i. (supplemental figure 4A).

The SPECT/CT scan of ^{111}In -28H1 in a healthy mouse at 72 h p.i. showed that the majority of the radioactivity was cleared from the circulation with little bone marrow uptake (figure 1B). Whole body distribution of the isotype-matched control antibody ^{111}In -DP47GS was similar (figure 1C), with the exception of a slower clearance from the circulation, resulting in some residual activity in the heart region at 72 h p.i (supplemental figure 4B). With the non-FAP-binding control antibody ^{111}In -DP47GS the inflamed joints could also be visualized (figure 1C), however, to a much lesser extent than with ^{111}In -28H1.

A strong correlation was found between tracer uptake and arthritis severity as demonstrated by quantitative analysis of the SPECT/CT scans at both 1 and 3 d p.i. (figure 2). Analysis revealed that at both time points the uptake (%ID) correlated well with the arthritis score (Spearman's ρ 0.87, $p=0.007$ and 0.89, $p=0.005$, 1 and 3 d, respectively). There was good retention of radioactivity in the inflamed joints over the 3 d period. For ^{111}In -DP47GS, no correlation between uptake and arthritis score was found (Spearman's ρ 0.51, $p=0.20$ and 0.42, $p=0.30$, 1 and 3 d, respectively).

PET/CT imaging

PET/CT images of healthy mice injected with ^{89}Zr -28H1 showed a similar whole body distribution as the SPECT/CT scans with ^{111}In -labeled 28H1. Excellent targeting of ^{89}Zr -28H1 to inflamed joints was observed, as illustrated by the PET/CT scans (figure 3). Healthy mice only displayed accumulation in the heart region as well as in the bone (supplemental figure 5).

PET/CT imaging was also performed with the clinically established radiotracer [^{18}F]FDG, a radiolabeled glucose analog, which accumulates in cells with increased glucose uptake such as tumor cells and inflammatory cells (mainly neutrophils). PET/CT imaging with [^{18}F]FDG showed low uptake in inflamed

joints (figure 3B). Only severely inflamed joints with a score above 1.25 were visualized, and signal intensity was much lower as compared to that found with the radiolabeled anti-FAP antibodies.

Biodistribution studies

Biodistribution studies of mice that received ^{111}In -labeled 28H1 revealed that the whole body distribution of the radioactivity in arthritic mice was similar to that in healthy mice. In line with the quantitative SPECT imaging data, accumulation of ^{111}In -28H1 in the inflamed joints correlated well with the arthritis score as shown in figure 4A (Spearman's p 0.69, $p<0.0001$). Highest joint uptake of the radiolabeled anti-FAP antibody was found in mice with severely inflamed joints with the maximum arthritis score of 2 (mean $25.9 \pm 4.2\text{ \%ID/g}$, range $19.0 - 32.1\text{ \%ID/g}$), whereas uptake in non-arthritic joints was significantly lower (mean $4.5 \pm 1.1\text{ \%ID/g}$, range $2.2 - 6.5\text{ \%ID/g}$; $P<0.0001$) (figure 4A).

Dissection revealed that uptake of ^{111}In -DP47GS in inflamed joints increased only slightly with increasing arthritis scores up to 0.75, but did not increase further in arthritic joints with scores from 0.75 – 2 (figure 4B). Uptake of ^{111}In -DP47GS in non-arthritic joints ranged from $1.6 - 8.4\text{ \%ID/g}$ (mean $3.5 \pm 1.4\text{ \%ID/g}$). Highest accumulation was found in joints with arthritis scores from 0.75 – 2 but never exceeded 12.0 \%ID/g (range $6.5 - 12.0\text{ \%ID/g}$, mean $9.8 \pm 1.6\text{ \%ID/g}$). The higher joint uptake of 28H1 as compared to the isotype-matched control antibody DP47GS, strongly indicates that the uptake in the arthritic joints was FAP-mediated.

Similar to the ^{111}In -labeled anti-FAP compound, uptake of ^{89}Zr -28H1 in inflamed joints also correlated with the arthritis score (figure 4C, Spearman's p 0.060, $p<0.0001$). Joint uptake of ^{89}Zr -28H1 in both normal and inflamed joints was higher than that of ^{111}In -labeled 28H1. This may partly be due to the higher bone uptake of ^{89}Zr as compared to that of ^{111}In . The biodistribution study after dissection (72 h

p.i.) revealed that femoral bone uptake of ^{89}Zr in arthritic mice was significantly higher than that of ^{111}In ($32.4 \pm 9.2\% \text{ID/g}$ vs. $5.1 \pm 0.4\% \text{ID/g}$, $p=0.0016$) (Supplementary data figure 3).

Interestingly, in mice injected with either $^{111}\text{In-28H1}$ or $^{89}\text{Zr-28H1}$, elevated uptake in the bone marrow was observed (supplementary data figure 3). $^{111}\text{In-28H1}$ showed a bone marrow uptake of $8.4 \pm 0.9\% \text{ID/g}$, whereas the uptake of $^{111}\text{In-DP47GS}$ was significantly lower ($4.8 \pm 1.8\% \text{ID/g}$, $P=0.018$), indicating that the bone marrow uptake was also FAP-mediated.

Uptake of $[^{18}\text{F}]$ FDG in non-inflamed joints was low (mean $3.3 \pm 2.4\% \text{ID/g}$, range $1.8 - 7.5\% \text{ID/g}$, figure 4D), whereas uptake in more severely inflamed joints was higher; joints with scores of 1.75 showed a mean uptake of $6.4 \pm 2.6\% \text{ID/g}$ (range $3.5 - 10.2\% \text{ID/g}$) and joints with a score of 2 showed a mean uptake was $9.1 \pm 4.5\% \text{ID/g}$ (range $3.9 - 11.7\% \text{ID/g}$).

Localization of the radioactivity in the affected knee joints was demonstrated by a high resolution scan of an affected knee of a mouse 3 days p.i. of $^{111}\text{In-28H1}$. Figure 5 shows that the radioactivity in the joint is localized in the synovial area of the femur-tibia region as well as the patella-femur region.

DISCUSSION

With SPECT and PET imaging, we demonstrated that radiolabeled anti-FAP antibodies specifically targeted to inflamed joints in an experimental model of rheumatoid arthritis. In addition, the present study showed that the uptake of the radiolabeled antibody correlated with the arthritis severity.

Until now, targeting of FAP with radiolabeled antibodies has been studied exclusively in tumor models since FAP is abundantly expressed on carcinoma-associated fibroblasts in the tumor stroma. Good and

specific targeting of tumor with ^{131}I -labeled murine F19 (9) and ^{131}I -labeled sibrotuzumab, a humanized version of the F19 antibody (10) has been demonstrated. However, due to lack of therapeutic effect as well as the occurrence of human-anti-human antibodies (HAHA), further clinical development of sibrotuzumab was halted. Engineering human Fab fragments into fully human IgG1 led to the development of two anti-FAP antibodies, ESC11 and ESC14. These rapidly internalizing, ^{177}Lu -labeled antibodies showed good tumor targeting as well as a significant therapeutic effect in melanoma xenografted mice (11).

Besides expression in tumor stroma and granulation tissue of healing wounds (4), FAP also is abundantly expressed by fibroblast-like synoviocytes in rheumatoid arthritis (2). It was also shown that expression of FAP was higher in RA than in osteoarthritis (OA). The authors speculated that the pronounced expression of FAP in RA might be related to the degree of synovial inflammation. Analyzing the gene expression profiles in inflamed paws of CIA mice confirmed that FAP expression was seven-fold increased in inflamed paws as compared to non-inflamed paws (17). Therefore, we hypothesized that imaging of FAP expression with 28H1 might be a valuable tool to assess the severity of the inflammation. Here, we demonstrated that the uptake of the anti-FAP antibody 28H1 increased with enhanced severity of inflammation. It is therefore anticipated that anti-FAP imaging might be a new sensitive tool for scoring RA disease activity, and could possibly be of additive value to existing scoring systems such as DAS28. Most importantly, it might allow noninvasive early therapy response monitoring.

The non-specific isotype-matched control antibody DP47GS also localized in inflamed joints, but the accumulation did not increase with increasing severity at higher scores. This led us to conclude that the major part of the uptake of 28H1 in inflamed joints was FAP-mediated. Enhanced uptake of DP47GS in

inflamed joints was due to locally enhanced vascular permeability at inflamed sites, resulting in extravasation of larger molecules such as antibodies, also known as the enhanced permeability and retention effect (18). This effect has been shown with ^{99m}Tc-labeled non-specific polyclonal IgG in a rat model of arthritis (19).

In the present study, imaging was performed with both ⁸⁹Zr and ¹¹¹In-labeled FAP antibody 28H1. Although the image quality was similar for both radionuclides, ⁸⁹Zr-28H1 had the disadvantage of enhanced uptake in the bone, most likely caused by unbound ⁸⁹Zr, released from the radiolabeled antibody after metabolism *in vivo*. This phenomenon has been described in previous studies with ⁸⁹Zr-anti-EGFR and anti-IGF1R antibodies (20, 21). Also others reported elevated bone uptake of ⁸⁹Zr compared to ¹¹¹In (21, 22). When imaging inflamed joints and bone-related disorders, this elevated bone uptake is unwanted and hampers the interpretation of the scans. Therefore, the use of ¹¹¹In for imaging with anti-FAP antibodies in rheumatoid arthritis is preferred over that of ⁸⁹Zr.

Radionuclide imaging in RA has been mainly focused on FDG PET/CT imaging (23), but also radiolabeled peptides such as IL1-ra , annexin-V and small molecules such as folate, PK11195, and MMP- and E-selectin-targeting molecules have been investigated both clinically and/or preclinically (24). In addition, radiolabeled antibodies such as anti-CD20 (rituximab) and anti-TNF α (infliximab) have been studied. Although these tracers accumulated specifically in affected joints, uptake could generally not be correlated with the severity of the inflammation. FDG has been studied extensively and joint accumulation has been proven to correlate with disease activity scores (25, 26), and we therefore also included [¹⁸F]FDG in our studies as a reference. However, uptake of FDG in arthritic joints in the CIA model was relatively low and did not correlate with the severity of the inflammation, which is in line with previous preclinical studies (27, 28), although one study reported a good correlation (29). These

differences might be explained by the use of various models, but also imaging might have been performed at various time-points after the onset of the arthritis. Therefore, FDG-PET imaging of experimental arthritis in mice is considered to be of limited value. Generally, neutrophils and activated macrophages mainly contribute to FDG uptake in inflammatory diseases. However, in rats with collagen-induced arthritis it was shown that increased accumulation was mainly caused by uptake in activated fibroblasts in the pannus, rather than by neutrophils (30).

We noted an unexpectedly high bone marrow uptake of the 28H1 anti-FAP antibody, which was not observed with the isotype-matched control antibody DP47GS. This indicates that the uptake was specific and most likely FAP-mediated. These findings corroborate with a recent study in which it has been described that both mouse and human pluripotent bone marrow stem cells could be recognized by FAP-reactive T-cells (31).

CONCLUSION

SPECT/CT imaging with the anti-FAP antibody ^{111}In -28H1 specifically visualized arthritic joints with high resolution, and accumulation correlated with the severity of the inflammation in murine experimental arthritis. Background uptake of the radiolabeled antibody was low, resulting in excellent image quality. Future studies will focus on the potential role of 28H1 as a tool to monitor therapy response early after the start of treatment.

ACKNOWLEDGEMENTS

The authors thank Anniek van der Waart, PhD, Department of Laboratory Medicine - Laboratory of Hematology, Radboud University Medical Center, Nijmegen, the Netherlands for expert help in analysis of bone marrow samples. Samantha Y.A. Terry was funded by the Roche Postdoc Fellowship (RPF) Program.

References

1. Firestein GS. Invasive fibroblast-like synoviocytes in rheumatoid arthritis. Passive responders or transformed aggressors? *Arthritis Rheum.* 1996;39:1781-1790.
2. Bauer S, Jendro MC, Wadle A, et al. Fibroblast activation protein is expressed by rheumatoid myofibroblast-like synoviocytes. *Arthritis Res Ther.* 2006;8:R171.
3. Scanlan MJ, Raj BK, Calvo B, et al. Molecular cloning of fibroblast activation protein alpha, a member of the serine protease family selectively expressed in stromal fibroblasts of epithelial cancers. *Proc Natl Acad Sci U S A.* 1994;91:5657-5661.
4. Grinnell F. Fibroblasts, myofibroblasts, and wound contraction. *J Cell Biol.* 1994;124:401-404.
5. Morimoto C, Schlossman SF. The structure and function of CD26 in the T-cell immune response. *Immunol Rev.* 1998;161:55-70.
6. Goldstein LA, Ghersi G, Pineiro-Sanchez ML, et al. Molecular cloning of seprase: a serine integral membrane protease from human melanoma. *Biochim Biophys Acta.* 1997;1361:11-19.
7. Garin-Chesa P, Old LJ, Rettig WJ. Cell surface glycoprotein of reactive stromal fibroblasts as a potential antibody target in human epithelial cancers. *Proc Natl Acad Sci U S A.* 1990;87:7235-7239.
8. Park JE, Lenter MC, Zimmermann RN, Garin-Chesa P, Old LJ, Rettig WJ. Fibroblast activation protein, a dual specificity serine protease expressed in reactive human tumor stromal fibroblasts. *J Biol Chem.* 1999;274:36505-36512.
9. Welt S, Divgi CR, Scott AM, et al. Antibody targeting in metastatic colon cancer: a phase I study of monoclonal antibody F19 against a cell-surface protein of reactive tumor stromal fibroblasts. *J Clin Oncol.* 1994;12:1193-1203.
10. Scott AM, Wiseman G, Welt S, et al. A Phase I dose-escalation study of sibrotuzumab in patients with advanced or metastatic fibroblast activation protein-positive cancer. *Clin Cancer Res.* 2003;9:1639-1647.

11. Fischer E, Chaitanya K, Wuest T, et al. Radioimmunotherapy of fibroblast activation protein positive tumors by rapidly internalizing antibodies. *Clin Cancer Res.* 2012;18:6208-6218.
12. Brom M, Joosten L, Oyen WJ, Gotthardt M, Boerman OC. Improved labelling of DTPA- and DOTA-conjugated peptides and antibodies with ^{111}In in HEPES and MES buffer. *EJNMMI Res.* 2012;2:4.
13. Verel I, Visser GW, Boellaard R, Stigter-van Walsum M, Snow GB, van Dongen GA. ^{89}Zr immuno-PET: comprehensive procedures for the production of ^{89}Zr -labeled monoclonal antibodies. *J Nucl Med.* 2003;44:1271-1281.
14. Joosten LA, Helsen MM, van de Loo FA, van den Berg WB. Anticytokine treatment of established type II collagen-induced arthritis in DBA/1 mice. A comparative study using anti-TNF alpha, anti-IL-1 alpha/beta, and IL-1Ra. *Arthritis Rheum.* 1996;39:797-809.
15. van der Have F, Vastenhouw B, Ramakers RM, et al. U-SPECT-II: An ultra-high-resolution device for molecular small-animal imaging. *J Nucl Med.* 2009;50:599-605.
16. Visser EP, Disselhorst JA, Brom M, et al. Spatial resolution and sensitivity of the Inveon small-animal PET scanner. *J Nucl Med.* 2009;50:139-147.
17. Ibrahim SM, Koczan D, Thiesen HJ. Gene-expression profile of collagen-induced arthritis. *J Autoimmun.* 2002;18:159-167.
18. Maeda H, Seymour LW, Miyamoto Y. Conjugates of anticancer agents and polymers: advantages of macromolecular therapeutics in vivo. *Bioconjug Chem.* 1992;3:351-362.
19. Boerman OC, Oyen WJ, Storm G, et al. Technetium-99m labelled liposomes to image experimental arthritis. *Ann Rheum Dis.* 1997;56:369-373.
20. Heskamp S, van Laarhoven HW, Molkenboer-Kuenen JD, et al. ImmunoSPECT and immunoPET of IGF-1R expression with the radiolabeled antibody R1507 in a triple-negative breast cancer model. *J Nucl Med.* 2010;51:1565-1572.

21. Perk LR, Visser GW, Vosjan MJ, et al. (89)Zr as a PET surrogate radioisotope for scouting biodistribution of the therapeutic radiometals (90)Y and (177)Lu in tumor-bearing nude mice after coupling to the internalizing antibody cetuximab. *J Nucl Med.* 2005;46:1898-1906.
22. Dijkers EC, Kosterink JG, Rademaker AP, et al. Development and characterization of clinical-grade 89Zr-trastuzumab for HER2/neu immunoPET imaging. *J Nucl Med.* 2009;50:974-981.
23. Kubota K, Ito K, Morooka M, et al. FDG PET for rheumatoid arthritis: basic considerations and whole-body PET/CT. *Ann N Y Acad Sci.* 2011;1228:29-38.
24. Mountz JM, Alavi A, Mountz JD. Emerging optical and nuclear medicine imaging methods in rheumatoid arthritis. *Nat Rev Rheumatol.* 2012;8:719-728.
25. van der Laken CJ, Huisman MH, Voskuyl AE. Nuclear imaging of rheumatic diseases. *Best Pract Res Clin Rheumatol.* 2012;26:787-804.
26. Roivainen A, Hautaniemi S, Mottonen T, et al. Correlation of 18F-FDG PET/CT assessments with disease activity and markers of inflammation in patients with early rheumatoid arthritis following the initiation of combination therapy with triple oral antirheumatic drugs. *Eur J Nucl Med Mol Imaging.* 2013;40:403-410.
27. Irmler IM, Opfermann T, Gebhardt P, et al. In vivo molecular imaging of experimental joint inflammation by combined (18)F-FDG positron emission tomography and computed tomography. *Arthritis Res Ther.* 2010;12:R203.
28. Cha JH, Lee SH, Lee SW, et al. Assessment of collagen-induced arthritis using cyanine 5.5 conjugated with hydrophobically modified glycol chitosan nanoparticles: correlation with 18F-fluorodeoxyglucose positron emission tomography data. *Korean J Radiol.* 2012;13:450-457.
29. Kundu-Raychaudhuri S, Mitra A, Datta-Mitra A, Chaudhari AJ, Raychaudhuri SP. In vivo quantification of mouse autoimmune arthritis by PET/CT. *Int J Rheum Dis.* 2014. doi: 10.1111/1756-185X.12410
30. Matsui T, Nakata N, Nagai S, et al. Inflammatory cytokines and hypoxia contribute to 18F-FDG uptake by cells involved in pannus formation in rheumatoid arthritis. *J Nucl Med.* 2009;50:920-926.

- 31.** Tran E, Chinnasamy D, Yu Z, et al. Immune targeting of fibroblast activation protein triggers recognition of multipotent bone marrow stromal cells and cachexia. *J Exp Med.* 2013;210:1125-1135.

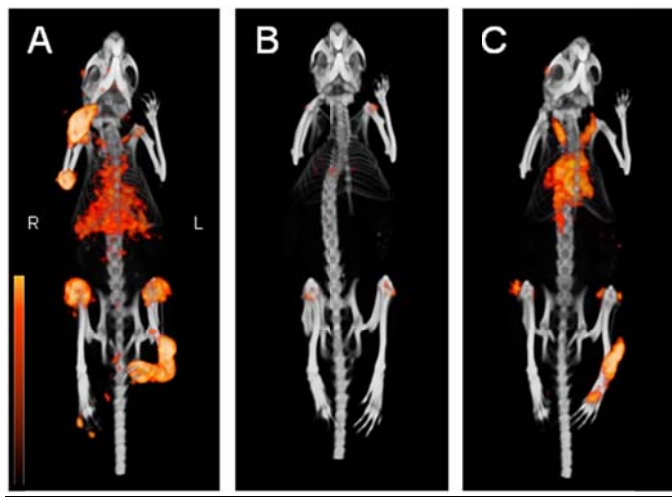


Figure 1. 3D SPECT/CT scans of mice with collagen-induced arthritis, injected with 15 MBq ^{111}In -labeled antibody (50 μg). ^{111}In -28H1 at 24 h p.i. (A) with joints scores of 1.75, 0, 0.25 and 1.5 (front right, front left, hind right, hind left, respectively). Radiotracer uptake is clearly visible in the inflamed joints. Panel B: ^{111}In -28H1 at 72 h p.i. in a healthy mouse. Some bone marrow uptake is visible. Panel C: ^{111}In -DP47GS at 24 h with joints scores of 0, 0, 2 and 0.5 (front right, front left, hind right, hind left, respectively). R and L indicate right and left side of mice, respectively. All images are scaled similarly.

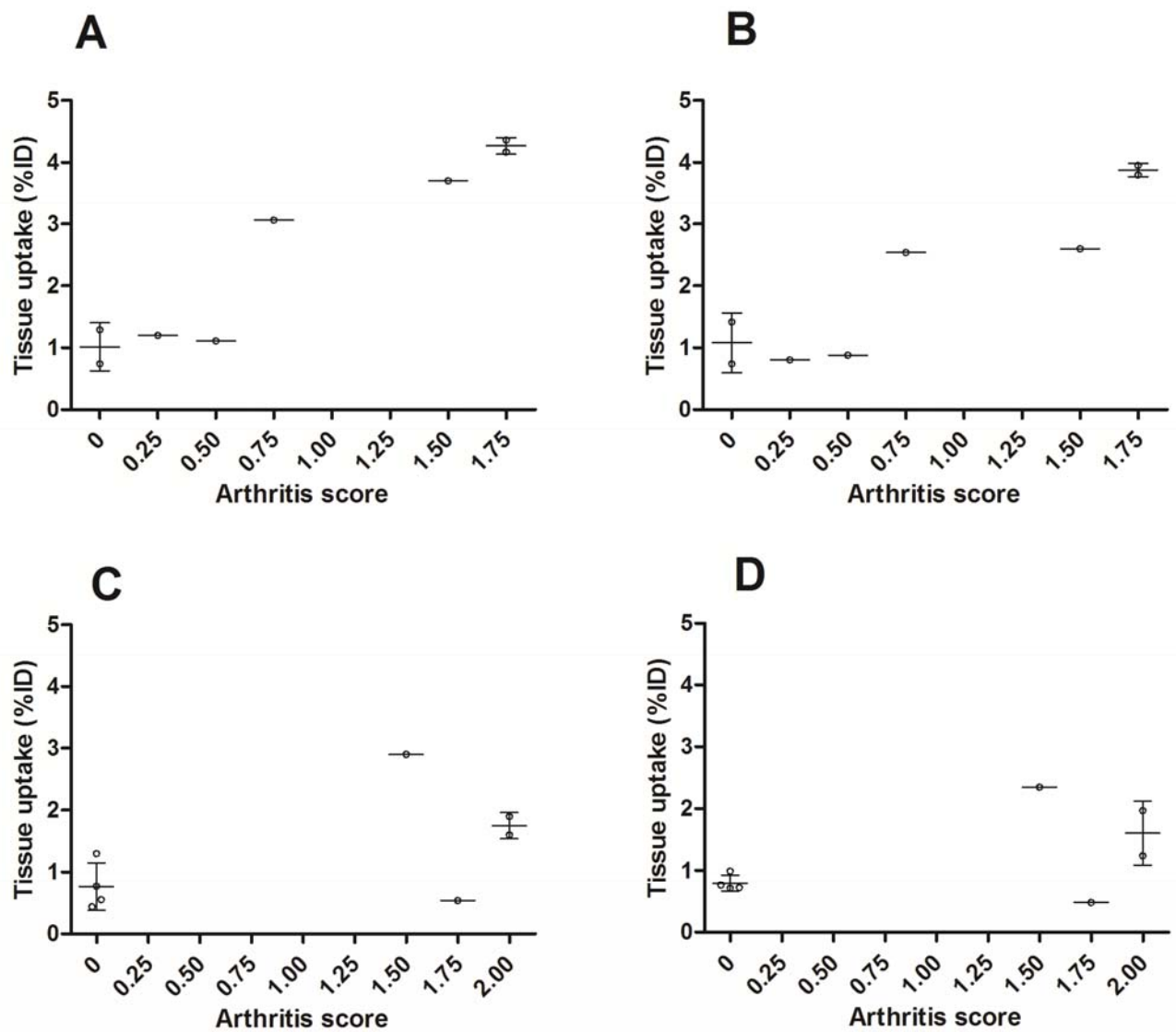


Figure 2. Joint uptake vs score of inflammation based on quantitative analysis of the SPECT scans of ^{111}In -28H1 after 1 d (A) and 3 d (B), and of ^{111}In -DP47GS after 1 d (C) and 3 d (D).

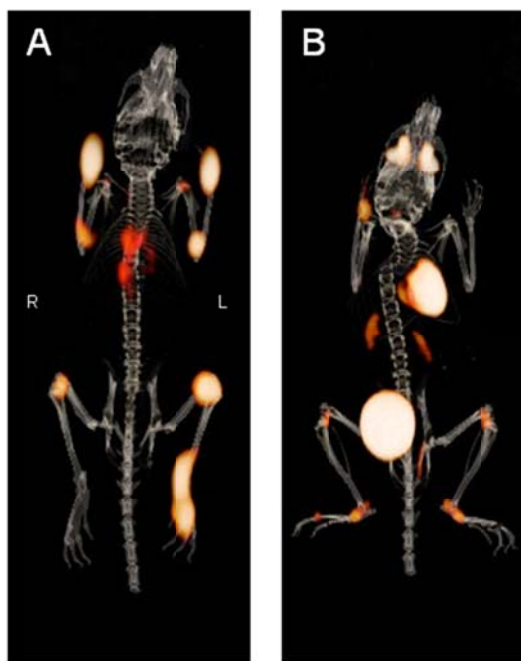


Figure 3. PET/CT scans (3D) of a mouse with collagen-induced arthritis, injected with 5 MBq ^{89}Zr -28H1 and scanned at 72 h p.i. (A). Joints scores were 1.75, 1.5, 0.25 and 2 (front right, front left, hind right, hind left, respectively). Right panel (B) shows a PET/CT scan of mouse with collagen-induced arthritis, injected with 10 MBq ^{18}F [FDG] and scanned at 1 h p.i. Joints scores were 0, 0.25, 1.25 and 0.25 (front right, front left, hind right, hind left, respectively). R and L indicate right and left side of mice, respectively.

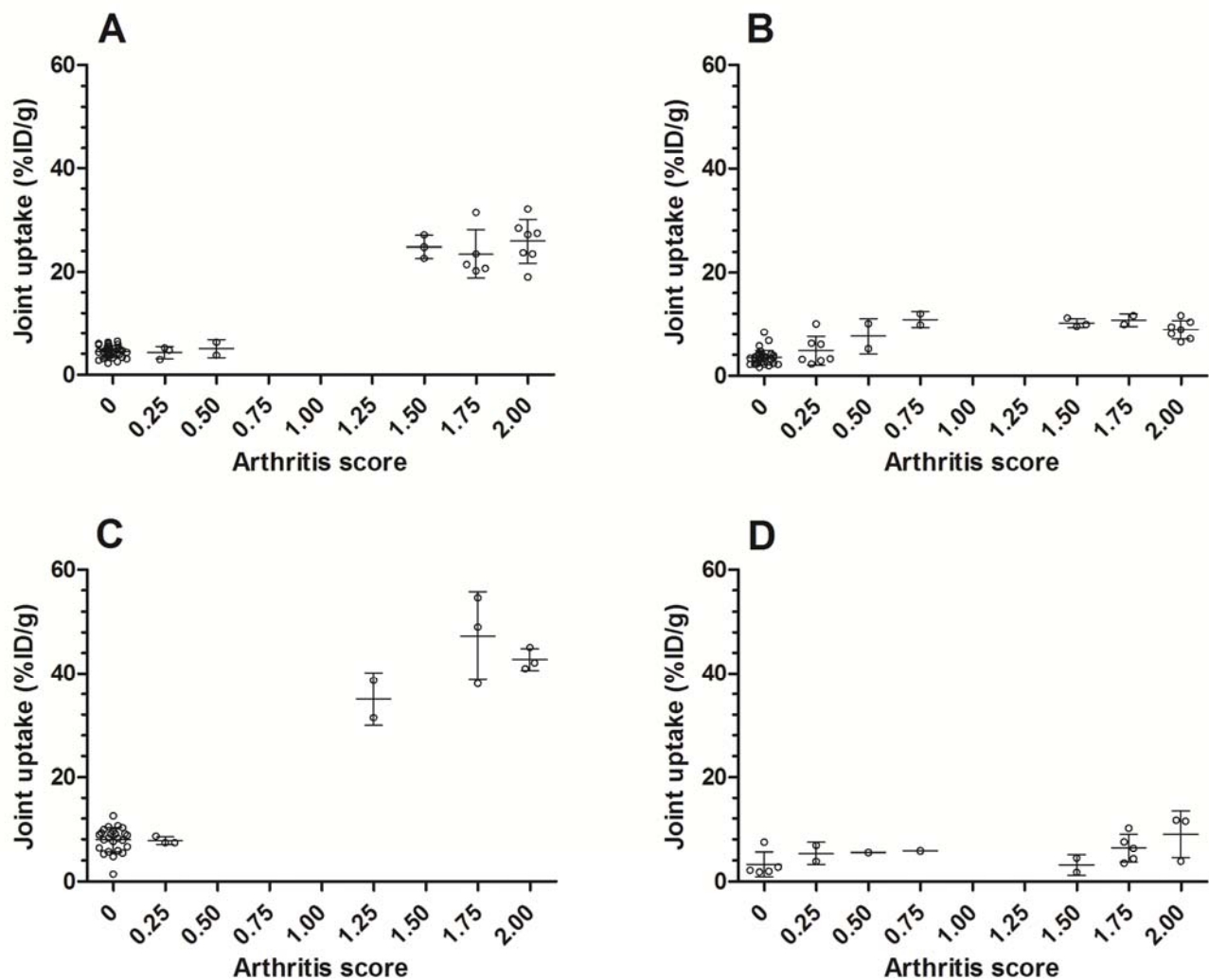


Figure 4. Joint uptake vs macroscopic score of arthritis of $^{111}\text{In}-28\text{H}1$ (A), $^{111}\text{In}-\text{DP}47\text{GS}$ (B), $^{89}\text{Zr}-28\text{H}1$ (C) and $[^{18}\text{F}]FDG$ (D). Joint uptake was measured in dissected tissues, 3 days p.i. of the radiolabeled antibodies.

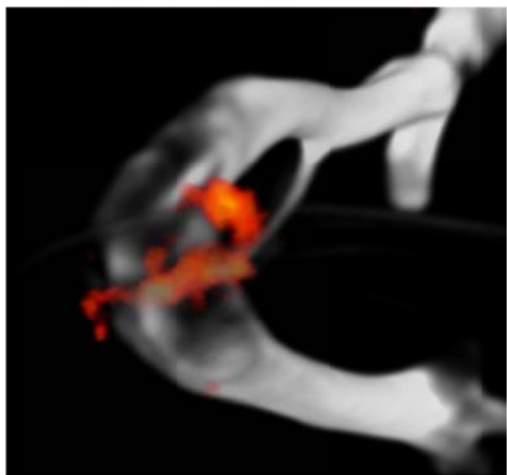


Figure 5. High resolution 3D SPECT/CT scan of a knee joint (score 0.75) of an arthritic DBA/1J mouse i.v. injected with ^{111}In -28H1 and scanned at 72 h p.i. Radioactivity was mainly localized to the synovial area of the femur-tibia and patella-femur region.